Send Orders for Reprints to reprints@benthamscience.ae

Current Nanoscience, **2015,** *11,* **253-260** **253**

Room Temperature Ammonia Gas Sensing Properties of Biosynthesized tin Oxide Nanoparticle Thin Films

Ketan P. Gattu[a], Kalyani Ghule[a], Anil A. Kashale[a], R.S. Mane[c], Ramphal Sharma[a], D.M. Phase[b], S.H. Han[c] and Anil Vithal Ghule[a,c,*]

[a]*Department of Nanotechnology, Dr. Babasaheb Ambedkar Marathwada University, Aurangabad 431004, Maharashtra, India;* [b]*UGC-DAE- Consortium of Scientific Research, Indore, (M.P), India;* [c]*Department of Chemistry, Hanyang University, Sungdong-Ku, Haengdang-dong 17, Seoul 133-791, Republic of Korea*

Abstract: Tin oxide (SnO_2) nanoparticles are prepared by simple and cost-effective biosynthesis method, wherein, tin chloride ($SnCl_4$) reacts with Bengal gram bean (*Cicer arietinum* L.) extract. The as-synthesized SnO_2 nanoparticles were coated onto the glass substrates using doctor blade method to form thin films. The films were further annealed at 250^oC and used for characterization and gas sensing applications. Alternatively, the SnO_2 nanoparticles were biosynthesized using carbohydrate (starch) and also by chemical precipitation method. A comparative study of structural and morphological properties of chemical and biosynthesized SnO_2 nanoparticles is also carried out. Further, room temperature ammonia gas sensing properties of the biosynthesized SnO_2 nanoparticles thin films are studied.

Keywords: Biosynthesis, electron microscopy, nanostructures, oxides, sensors.

1. INTRODUCTION

Ammonia (NH_3) assumes an essential part in all manifestations of life and is the second most widely utilized chemical in the world [1]. It is intensely dangerous, if breathed in over the moderate amount [2]. Thus, ammonia sensors stay the potential candidates used in agriculture, chemical, pharmaceutical, and food process industries to detect the NH_3 leak in controlled atmospheres [3]. Range of NH_3 sensors based on optical fibres [4], potentiometric electrodes [5], conducting polymers [6], infrared devices and metal oxides [3, 7, 8] has been developed. However, developing efficient room temperature operated sensors still remains a potential challenge, creating interest among researchers to make the device portable, with increased long-term stability and reduced power consumption. Attempts made to develop room temperature operated sensors include, sensors based on polyaniline (PANI) blend films [9, 10], graphene/PANI nanocomposites [11], (PANI/TiO_2) [12, 13], CNTs [14-16], SnO_2 [17, 18], SnO_2/CNT [19], Cellulose–TiO_2–MWCNT [20], (SnO_2–ZnO)/PPy [21], etc. Among these, the polymer based sensors (e.g. PANI) suffer from issue like long term stability. On the other hand, the composite based sensors (e.g. SnO_2/CNT) operating at room temperatures is expensive as their fabrication needs sophisticated instruments and expertise [22-27]. However, metal oxide sensors are inexpensive, have long term stability and can be efficient room temperature gas sensors by controlling particle size, increasing the surface area and surface composition of the metal oxide [28-30].

SnO_2 is one of the promising metal oxide semiconductor gas sensing materials with sensible gas response to numerous varieties of poisonous gases and organic vapours [31-40]. Specifically, SnO_2-based gas sensors can detect NH_3 gas with good sensitivity and response-recovery time [26, 41, 42]. A variety of ways for the preparation of SnO_2 nanoparticles have been proposed viz. magnetron sputtering, sol–gel, chemical vapour deposition, thermal evaporation etc. However, the preparations are carried out at high temperatures using these techniques. As a result, the particle size increases thereby decreasing the surface area because of sintering.

Recently, biosynthesis has received attention in the field of material synthesis, particularly in metal oxides based materials [43-46]. These methods use raw materials which are abundant, inexpensive and renewable and have biological and chemical properties such as non-toxicity, biocompatibility, biodegradability, polyfunctionality, hydrophilicity, high chemical reactivity, chirality, chelation adsorption abilities, etc. Thus, it opens enormous prospects in solution routes for the synthesis of nanomaterials. The biomolecules used for the synthesis act as (i) reducing/oxidizing agents (ii) stabilizing agents to regulate particle size by preventing agglomeration of nanoparticles, (iii) templates for directing particle growth and controlling structure and (iv) as surface functionalizing agents of the metal oxides, permitting their attachment and self-assembly on surfaces, an important property for loading desired biomolecules. Furthermore, we obtain narrow particle size distribution and a very small size of the

*Address correspondence to this author at the Department of Nanotechnology, Dr. Babasaheb Ambedkar Marathwada University, Aurangabad 431004, Maharashtra, India; Tel: +91-9730283381, +91-240-2403254; +91-240-2403284; E-mail: anighule@gamil.com

1875-6786/15 $58.00+.00

particles, as there is homogenous dispersion of the cations within the biomaterial and their low thermal degradation temperature leads to the formation of a larger number of smaller crystals of oxide material [44]. Along with this, there are reports on biomolecules-inorganic composite gas sensors with improved gas sensitivity [20, 47-48], making biosynthesis method possible. Thus, with this motivation, here we report an economic and efficient approach for fabricating biosynthesized SnO_2 based gas sensor device working at room temperature. The SnO_2 nanoparticles thin film gas sensors have been prepared by simple cost effective biosynthesis of SnO_2 nanoparticles, wherein tin chloride ($SnCl_4$) is reacted with Bengal gram bean (*Cicer arietinum* L.) extract. The present article focuses on the surface morphology and compositional property studies of biosynthesized SnO_2 thin films followed by room temperature ammonia gas sensing studies.

2. MATERIALS AND METHODS

In typical synthesis of tin oxide nanoparticles, 20 g of dry Bengal gram beans (*Cicer arietinum* L.) was soaked in 100 mL of DI water for 6 h at room temperature. Thereafter, the soaked seeds were removed and the extract was filtrated using a glass-fiber filter (GF/F) to be free from particulate matter. 10 mL of aqueous $SnCl_4$ (0.01 M) solution was added to 10 mL of the gram bean extract and diluted to 50 mL. The solution was centrifuged and the powder so obtained was calcined at 600°C to remove the organic contaminants. This powder was then thoroughly mixed with polyethylene glycol as a binder and coated onto the precleaned glass substrates to form thin films using the doctor blade method [49]. The coated thin films were then dried at room temperature and calcined at 450°C in air for 1 h to remove the binder and were used for further characterization and gas sensing application.

On the other hand, SnO_2 nanoparticles were synthesized by similar procedure using carbohydrates (starch) instead of gram bean extract to ensure the contribution of carbohydrates in the synthesis of tin oxide. For this 10 mL of aqueous $SnCl_4$ (0.01 M) solution was added to 10 mL of the starch solution (50 gm/L) under continuous stirring [50]. The solution was then centrifuged to obtain powder which was further calcined at 600°C to remove the starch. Alternately, tin oxide nanoparticles were also synthesized using chemical route (chemical precipitation) for comparison between the methods of synthesis and to study the quality of SnO_2 nanoparticles. For chemical synthesis of the SnO_2 nanoparticles, ammonia solution was drop wise added to 10 mL of aqueous $SnCl_4$ (0.01 M) solution under continuous stirring to obtain a pH of ~7-8 [51]. The white precipitate obtained was then centrifuged, rinsed and dried at room temperature and further calcined at 600°C. The SnO_2 nanoparticles so produced by these different methods were characterized for their preliminary structural and morphological properties. However, gas sensing properties of the biosynthesized SnO_2 nanoparticles thin film were studied in detail and its sensitivity for NH_3 gas was investigated in this work.

The biosynthesized nanocrystalline SnO_2 nanoparticles were investigated using X-ray diffraction (XRD). The XRD spectra of the SnO_2 nanoparticles (powder form) and also in thin film form were recorded using (MPD 1880, Philips, Japan) Advanced Powder X-ray Diffractometer (Cu $K\alpha_1$ = 1.54056 Å radiation). The SnO_2 nanoparticles thin films prepared by Dr. Blade method were sputter coated with platinum prior to their characterization using scanning electron microscopy (SEM, JEOL, Japan) to avoid charging effect. X-ray photoelectron spectroscopy (XPS) analysis was carried out using VG multilab ESCA 2000 system, using a monochromated MgKα source (1.254 keV). On the other hand, the separated biosynthesized SnO_2 nanoparticles were drop-coated onto the lacey carbon coated Cu grid and dried prior to TEM analysis using field emission transmission electron microscope (TEM, JEOL, JEM 2010F). Selected individual molecules viz. carbohydrate, ascorbic acid, pantothenic acid, niacin, choline, pyridoxine, riboflavin, biotin, vitamin K, β-carotene, inositol and tocopherol in the extract were identified using an electrospray ionization/ion trap mass spectrometer (ESI-MS, LCQ^{TM} DUO, ThermoFinnigan) controlled by Xcalibur^{TM} 1.1 software used for the analysis of the molecules present in the extract. The ESI voltage, capillary voltage, and tube lens offset were kept at 4.5 kV, 45 V and 40 V, respectively. The sheath gas was maintained at 50 arbitrary units. The capillary temperature was kept at 200 ^{o}C. Extract sample diluted 100 times using methanol with 0.1% ammonium acetate was introduced using direct injection mode and the ion trap was scanned from *m/z* 150 to *m/z* 2000 for full scan spectrum.

The thin films of biosynthesized SnO_2 nanoparticles were tested for ammonia gas sensing at room temperature using homemade gas sensing unit [52, 53] and silver metal contacts. The gas sensing unit consists of a bell jar situated over a brass plate having proper gas-in and gas-out connections. Fig. (**1**) shows the setup of homemade gas sensor unit. It consists of a borosil bell jar, a resistive connection with a precise temperature controller for maintaining the operating temperature, proper gas in and gas out system and a digital regulated voltage source. The change in current was recorded with the help of a pico ammeter and a rotary pump was used for gas out purpose. The thin films with silver metal contacts were placed within the test chamber of known volume. A fixed volume (200 ppm) of NH_3 gas was injected into the test chamber and film current at constant voltage was measured with reference to time, until it reached a steady value. The procedure was repeated after removing NH_3 and exposing the thin films to clean air. These steps were repeated for different NH_3 gas concentrations (200-600 ppm).

3. RESULTS AND DISCUSSION

3.1. Synthesis Mechanism

The biomolecules such as carbohydrates, proteins and lipids possessed by the gram bean [47] extract are expected to play an important role as (i) reducing/oxidizing agents (ii) stabilizing agents and (iii) templates, leading to the formation of SnO_2 nanoparticles in solution [17]. The exact mechanism for the synthesis of SnO_2 nanoparticles is not clear and the study is underway. To understand the contribution of biomolecules that are responsible for the synthesis of SnO_2 nanoparticles, we also used carbohydrate (starch) instead of using gram been extract for the synthesis

Fig. (1). Homemade gas sensing unit.

of SnO_2 nanoparticles. The carbohydrates spread within the extract behave like an organic template, binding several metal cations, through their functional groups (viz. carboxyl, hydroxyl or amino groups). This initial binding of the metal ions to the saccharide determines a uniform dispersion of the cations in well confined areas. Along with this, the low thermal degradation temperature of carbohydrates [54, 55] leads to the formation of a larger number of smaller crystals of oxide material, thus retaining small size [44] with the help of stabilizing biomolecules present in the extract. The presence of selected molecules like ascorbic acid, pantothenic acid, niacin, choline, pyridoxine, riboflavin, biotin, vitamin K, β-carotene,

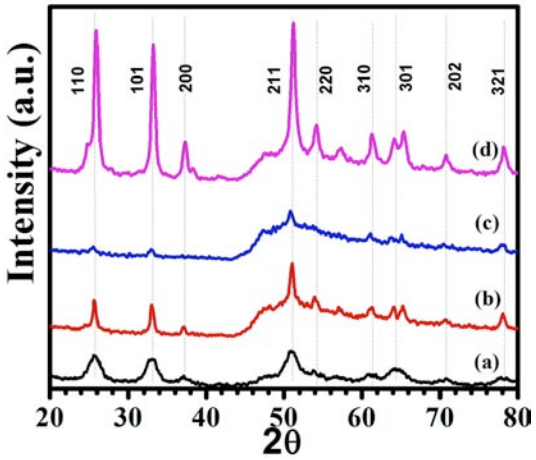

Fig. (2). Representative XRD spectra of SnO_2 nanoparticles (a) bio-synthesized (gram been extract mediated) (b) chemical synthesized (c) bio-synthesized (carbohydrate mediated) (d) bio-synthesized (gram been extract mediated) calcined at 600°C.

inositol, and tocopherol in the extract in addition to carbohydrates was confirmed by selected ion monitoring $[M+H]^+$, $[M+NH_4]^+$, and $[M+Na]^+$ mass spectrometry (data not shown).

3.2. Structural Studies

Crystal structure, phase and particle size of the product were determined using XRD patterns obtained from the samples. XRD spectra of the products are shown in Fig. (**2**). The diffraction peaks in Fig. (**2**) were indexed to represent the rutile phase of the SnO_2 with calculated lattice parameters been shown in Table **1**, which are consistent with the literature reported values (a = 4.775 Å, c = 3.199 Å, JCPDS No. 77-0447), and can be attributed to the space group P42 /mnm. The high purity of the final product was confirmed by the absence of any peaks due to the metallic tin or any other Sn based oxide or hydroxide. The average grain size of the product was determined from XRD peaks using Scherrer's formula $D=K\lambda/\beta\cos\theta$, where K is the Scherrer's constant (K= 0.9), λ is the wavelength of the incident X- rays, β is the full width at half maximum of the XRD peaks expressed in radian. The lattice parameters for tetragonal structure were calculated by

$$d_{hkl} = \frac{1}{\sqrt{\frac{h^2+k^2}{a^2}+\frac{l^2}{c^2}}} \quad (1)$$

Table 1. Lattice parameters and average grain size of SnO_2 nanoparticles synthesized using different methods.

Sr.No.	Synthesis Method	Average Grain Size	Lattice Parameters (Å)	
			a	c
1	Biosynthesis Method	6nm	4.81	3.29
2	Chemical co-precipitation	15nm	4.82	3.21
3	Starch Mediated	13nm	4.82	3.23
4	Biosynthesis Method (Calcined 600°C)	12nm	4.81	3.29

Where h, k, l are all integers, (hkl) is the lattice plane index, a and c are lattice constants.

From Table **1**, we can see that the average grain size of the bio-synthesized (gram bean extract mediated) SnO_2 nanoparticles is much smaller compared to carbohydrate (starch) mediated and chemically synthesized SnO_2 nanoparticles.

3.3. Scanning Electron Microscopy

Fig. (**3**) shows representative FE-SEM image of bio-synthesized SnO_2 nanoparticles thin film coated onto the glass substrate. The SEM profile as shown in Fig. (**3**) indicates fine granular surface of tin oxide coated over the entire glass substrate with no clusters formed by the agglomeration of finer particulates, which is in contrast to the case of metal oxide films deposited by chemical methods [56, 57]. Thus, the small particle size leading to the higher surface area obtained in biosynthesis is favourable for gas sensing [58]. The SEM image shows uniform size distribution of the SnO_2 nanoparticles. It can also be seen that the average grain size of the nanoparticles is below 10 nm, which is in good agreement with the XRD data.

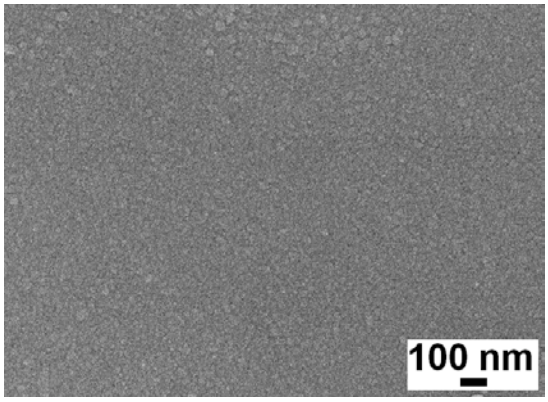

Fig. (3). Representative FESEM image of biosynthesized SnO_2 nanoparticles coated onto the glass substrate using doctor blade method.

3.4. Transmission Electron Microscopy

Fig. (**4**) shows the representative transmission electron microscopy (TEM) image of the biosynthesized SnO_2 nanocrystallites. The as-synthesized SnO_2 nanoparticles were observed to be monodispersed and the size was noted to be ~6 nm showing narrow size distribution (Figure not shown). Interestingly, no aggregation of SnO_2 nanoparticles was observed and the connected crystallites of ~10 nm formed a random network on calcination (Fig. **4**). The selected area electron diffraction pattern (SAED) pattern (inset in Fig. **4**) was obtained to investigate the crystallinity. It is observed that the SAED pattern obtained from the nanoparticles showed the diffused ring like pattern, which confirms the polycrystalline nature of the biosynthesized nanoparticles. It clearly shows the growth of nanoparticles along 110, 101, 211, 301 planes which is in agreement with the XRD data.

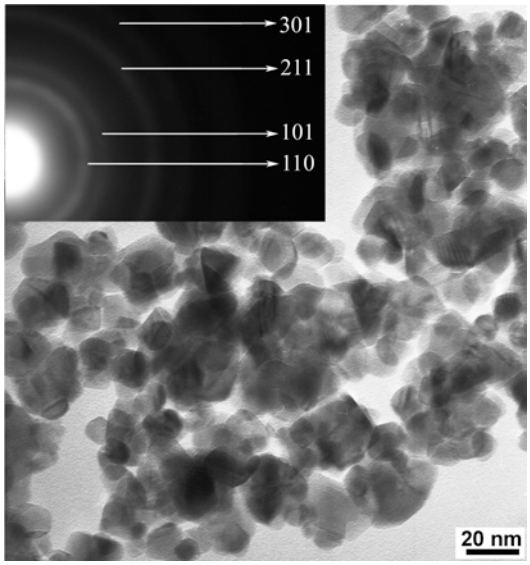

Fig. (4). Representative TEM image of biosynthesized SnO_2 nanoparticles and the inset shows SAED pattern.

3.5. XPS Analysis

Elemental composition and purity of the product are studied by X-ray Photoelectron Spectroscopy (XPS). The survey spectrum of the product (Fig. **5**) indicates high purity of SnO_2, since only Sn- and O-related core levels are detectable, apart from a weak C 1s peak at about 285 eV. The presence of carbon is mainly due to exposure of the sample to air. High-resolution characteristic spectra of Sn 3d, C 1s and O 1s are shown as inset in Fig. (**5**) as Fig. (**5a**, **b** and **c**), respectively. The Sn $3d_{5/2}$ and $3d_{3/2}$ peaks show a very symmetric line shape fitted by a single component with a binding energy of 486 eV and 495 eV, respectively. On the other hand, no peak corresponding to Sn^{2+} was detected, which confirmed the existence of SnO_2. The O 1s peak at 530 eV is attributed to Sn oxidation indicating that the product is nothing but SnO_2.

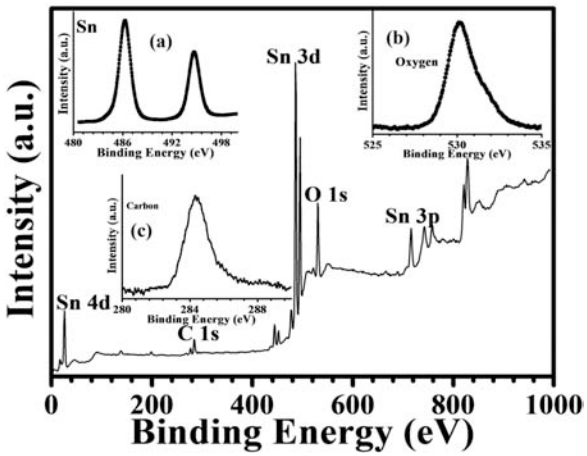

Fig. (5). XPS spectra of bio-synthesized SnO_2 nanoparticles. Inset **a**) Sn $3d_{5/2}$ and Sn $3d_{3/2}$ spectrum **b**) O 1s spectrum and **c**) C 1s spectrum.

3.6. Gas Sensing Studies: NH_3 Sensing Mechanism

When tin oxide nanoparticle thin films are exposed to ammonia gas, the pre-adsorbed oxygen over SnO_2 surface and NH_3 molecules interact with each other and release electrons to SnO_2. The interaction of pre-adsorbed oxygen and NH_3 molecules on the surface of SnO_2 is indicated in Eqs:

$$O_2 gas \xrightarrow{SnO_2+air} O_2(ads)$$

$$O_2(ads) + e^- \xrightarrow{SnO_2+air} O_2^-(ads)$$

$$O_2^-(ads) + e^- \xrightarrow{SnO_2+air} 2O^-(ads)$$

$$NH_3(gas) \leftrightarrow NH_3(ads) \quad (1)$$

$$2NH_3(ads) + 3O^-(ads) \leftrightarrow N_2 + 3H_2O + 3e^- \quad (2)$$

The release of electrons to SnO_2 results in an increase of carries, thus leading to an increase in surface conductivity of SnO_2 thin film and decrease in the barrier height at the grain boundaries between the nanocrystallites.

Fig. (**6a**) shows the schematic of the sensing mechanism involving adsorption of oxygen species on the surface of tin oxide nanoparticles, which abstract electrons, and thus, cause an increase in potential barrier at the grain boundaries. The gas molecules interact with the oxygen species and produce notable change in electronic property of the material. Thus, the density of oxygen species on the surface defines the rate of reaction and catalytic property. "In case of a catalytic reaction, the ammonia gas is first adsorbed on a catalyst, gets split up into ions and then spills over on the surface and reacts with surface oxygen ions of functional material, thereby decreasing the resistance of the sensor and enhancing the response" [59, 60]. The Fig. (**6b**) shows the schematic demonstrating change of the sensor resistance upon exposure to the target gas. Under ambient conditions, the electrons in the conduction band of the tin oxide nanoparticles are removed by the adsorbed oxygen ions. This causes a decrease in the carrier concentration, thereby increasing resistance at the operating temperature. When the sensor is exposed to NH_3 gas, the electrons gained from the chemical reaction are given back to the conduction band leading to the decrease in sensor resistance [59].

Ammonia Sensing Properties

Fig. (**7a**) shows the I-V curve obtained from biosynthesized SnO_2 nanoparticles thin film maintained at room temperature, before and after insertion of NH_3 gas and on exposure for various time intervals recorded with the bias voltage (+3V, -3V). Significant change in current is noted with variation in exposure time, justifies its sensitivity. Fig. (**7b**) shows the change in current as a function of time obtained from SnO_2 thin-film on exposure to ammonia atmosphere with a varying ammonia concentration (200, 300, 400 ppm). "The response and recovery time of a sensor can be defined as the time required for a film resistance to reach 90% of its saturation value from the starting value, from the time of gas exposure and on the removal of the gas, respectively" [53]. Here, the response and recovery time for SnO_2 thin-film were found to be ~6 and 8 s, respectively. "Response is defined as the ratio of the current in the gas atmosphere versus the current in air atmosphere" [61].

$$\frac{I_g}{I_a} = \text{Response}$$

Fig. (**7c**) shows the gas response curve as a function of gas concentration (200–600 ppm). Increasing trend and good linearity in the gas response curve is noted with the increase in the ammonia concentration (200- 600 ppm). This is probably attributable to the very fact that the amount of NH_3 molecules reacting with the O^- species increase with

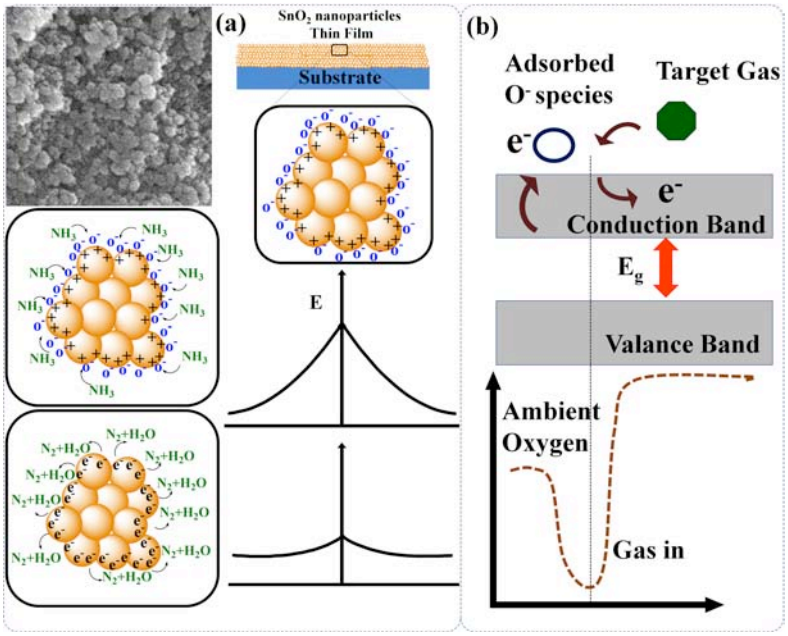

Fig. (6). a) Gas sensing mechanism of SnO_2 nanoparticles thin film on exposure to ammonia gas. **b**) Schematic showing electron transfer and change in electrical signal (resistance) upon exposure to the ammonia gas.

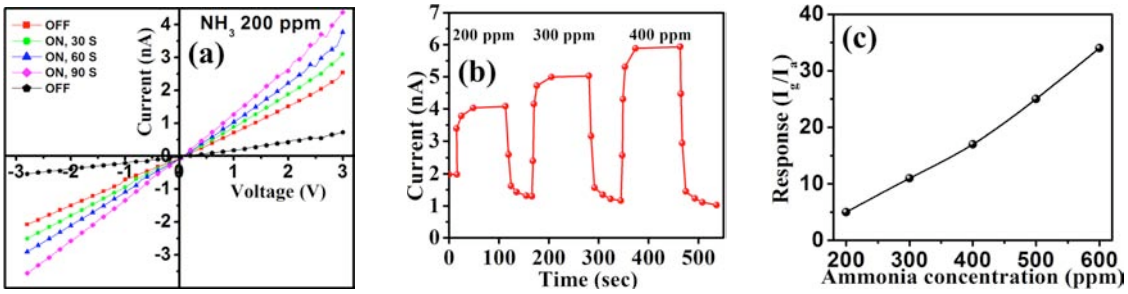

Fig. (7). a) I-V curve for bio-synthesized SnO_2 nanoparticles thin film (maintained at room temperature), before and after insertion of NH_3 gas at various time intervals. **b**) Change in current as a function of time with SnO_2 thin-film being exposed to varying ammonia concentration. **c**) Response curve as a function of varying ammonia concentration.

Table 2. Comparative table for SnO_2 gas sensors.

Sensor	Synthesis Method	Gas Detected	Operating Temperature	Gas Concentration	Response	Ref.
SnO_2	Biosynthesis	Ammonia	Room Temperature	600ppm	~34	
SnO_2	Dissolution pyrolysis	Ethanol	350 °C	50ppm	~500	[63]
SnO_2	Sol-gel	Ethanol	350 °C	1000ppm	~10	[64]
SnO_2	Hydrothermal	Ammonia	300 °C	800ppm	~200	[65]
SnO_2	Precipitation	Ethanol	250 °C	200ppm	~90	[66]
SnO_2 SWNT composite	Arc discharge	Ammonia	Room Temperature	60ppm	~40	[67]

increase in gas concentration. The ammonia gas with varying concentrations (200 ppm and 600 ppm) was inserted consecutively into the test chamber. With 200 ppm of ammonia, the response was found to be nearly 5 (Fig. **7c**), followed by very good recovery on the withdrawal of gas from the test chamber. Similarly, with 600 ppm of ammonia, the sample exhibited stable and reproducible response of 34 (Fig. **7c**). Linear response was noted from 200 ppm of ammonia extending up to 600 ppm. Interestingly, the gas sensing studies were explored at room temperature and the results were promising considering the fact that the SnO_2 particles were small with minimum to no aggregation, which increased the surface area and improved the sensing efficiency. A comparative table of SnO_2 gas sensors fabricated using various methods [62-66] and their gas response is shown in Table **2**. From Table **2**, we can clearly see that a higher response is either obtained at higher operating temperatures (~250-300°C) or is gained by using expensive sophisticated methods of synthesis of SnO_2 nanocomposites. On the contrary, the biosynthesised SnO_2 nanoparticles thin film show promising gas sensing results at room temperature and further studies are underway to improve the sensitivity of the gas sensors.

CONCLUSIONS

Tin oxide nanoparticles have been successfully biosynthesized by treating tin chloride ($SnCl_4$) with Bengal Gram bean extract, which were eventually coated onto the glass substrates using the doctor blade method. The morphological studies confirmed the uniform coating of the nanostructured SnO_2 over the entire surface of the substrate. The nanocrystalline nature of the SnO_2 film is confirmed from SAED pattern. The SnO_2 nanostructures probably increased the surface area, and thus the interaction between the ammonia gas and the sensing material, i.e. SnO_2 nanocrystallites on the thin-film. Considering all the above facts, the observed response of the biosynthesized SnO_2 nanoparticles thin-film at room temperature and at low concentration of gas is attributed to the small size of the particles, structure and surface morphology of the film due to the biosynthesis method contributing towards green nanotechnology.

CONFLICT OF INTEREST

The authors declare that the article content has no conflict of interest.

ACKNOWLEDGEMENTS

The authors are thankful to UGC-DAE Consortium for Scientific Research, Indore (Project Ref. No.: CSR-I/CRS-48/48) and UGC, New Delhi (F. No. 41-370/2012 (SR)) for the financial support. We are also thankful to the Department of Nanotechnology, Dr. Babasaheb Ambedkar Marathwada University, Aurangabad for providing the laboratory facility.

REFERENCES

[1] Erisman, J.W.; Sutton, M.A.; Galloway, J.; Klimont, Z.; Winiwarter, W. How a century of ammonia synthesis changed the world. *Nat. Geosci.*, **2008**, *1*, 636-639.

[2] Occupational Safety & Health Administration Ammonia in Workplace Atmospheres - Solid Sorbent. https://www.osha.gov/dts/sltc/methods/inorganic/id188/id188.html.

[3] Timmer, B.; Olthuis, W.; van den Berg, A. Ammonia sensors and their applications - a review. *Sens. Actuator B-Chem.*, **2005**, *107*, 666-677.

[4] Chambers, P.; Lyons, W.B.; Lewis, E.; Sun, T.; Grattan, K.T.V. The potential for development of an NH_3 optical fibre gas sensor. *J. Phys. Conf. Ser*., **2007**, *85*, 012015.

[5] Meyerhoff, M.E.; Fraticelli, Y.M.; Greenberg, J.A.; Rosen, J.; Parks, S.J.; Opdycke, W.N. Polymer-membrane electrode-based potentiometric sensing of ammonia and carbon dioxide in physiological fluids. *Clin. Chem.*, **1982**, *28*, 1973-1978.

[6] Choi, H.; Lee, J.; Dong, K.-Y.; Ju, B.-K.; Lee, W. Gas sensing performance of composite materials using conducting polymer/single-walled carbon nanotubes. *Macromol. Res.*, **2012**, *20*, 143-146.

[7] Xi, L.J.; Qian, D.; Tang, X.C.; Chen, C.J. High surface area SnO_2 nanoparticles: Synthesis and gas sensing properties. *Mater. Chem. Phys*., **2008**, *108*, 232-236.

[8] Thong, L.V.; Hoa, N.D.; Le, D.T.T.; Viet, D.T.; Tam, P.D.; Le, A.-T.; Hieu, N.V. On-chip fabrication of SnO_2-nanowire gas sensor: The effect of growth time on sensor performance. *Sens. Actuator B-Chem.*, **2010**, *146*, 361-367.

[9] Li, Y.H.; Gong, J.A.; He, G.H.; Deng, Y.L. Synthesis of polyaniline nanotubes using Mn_2O_3 nanofibers as oxidant and their ammonia sensing properties. *Synth. Met.*, **2011**, *161*, 56-61.

[10] Matsuguchi, M.; Io, J.; Sugiyama, G.; Sakai, Y. Effect of NH_3 gas on the electrical conductivity of polyaniline blend films. *Synth. Met.*, **2002**, *128*, 15-19.

[11] Wu, Z.Q.; Chen, X.D.; Zhu, S.B.; Zhou, Z.W.; Yao, Y.; Quan, W.; Liu, B. Enhanced sensitivity of ammonia sensor using graphene/polyaniline nanocomposite. *Sens. Actuator B-Chem.*, **2013**, *178*, 485-493.

[12] Li, Y.H.; Gong, J.; He, G.H.; Deng, Y.L. Fabrication of polyaniline/titanium dioxide composite nanofibers for gas sensing application. *Mater. Chem. Phys.*, **2011**, *129*, 477-482.

[13] Tai, H.L.; Jiang, Y.D.; Xie, G.Z.; Yu, J.S. Preparation, characterization and comparative NH_3-sensing characteristic studies of PANI/inorganic oxides nanocomposite thin films. *J. Mater. Sci. Technol.*, **2010**, *26*, 605-613.

[14] Wang, S.G.; Zhang, Q.; Yang, D.J.; Sellin, P.J.; Zhong, G.F. Multi-walled carbon nanotube-based gas sensors for NH_3 detection. *Diam. Relat. Mater*., **2004**, *13*, 1327-1332.

[15] Kong, J.; Franklin, N.R.; Zhou, C.; Chapline, M.G.; Peng, S.; Cho, K.; Dai, H. Nanotube molecular wires as chemical sensors. *Science*, **2000**, *287*, 622-625.

[16] Arab, M.; Berger, F.; Picaud, F.; Ramseyer, C.; Glory, J.; Mayne-L'Hermite, M. Direct growth of the multi-walled carbon nanotubes as a tool to detect ammonia at room temperature. *Chem. Phys. Lett.*, **2006**, *433*, 175-181.

[17] Bekyarova, E.; Davis, M.; Burch, T.; Itkis, M.E.; Zhao, B.; Sunshine, S.; Haddon, R.C. Chemically functionalized single-walled carbon nanotubes as ammonia sensors †. *J. Phys. Chem. B*, **2004**, *108*, 19717-19720.

[18] Kovalenko, V.V.; Zhukova, A.A.; Rumyantseva, M.N.; Gaskov, A.M.; Yushchenko, V.V.; Ivanova, I.I.; Pagnier, T. Surface chemistry of nanocrystalline SnO_2: Effect of thermal treatment and additives. *Sens. Actuator B-Chem.*, **2007**, *126*, 52-55.

[19] Van Hieu, N.; Thuy, L.T.B.; Chien, N.D. Highly sensitive thin film NH_3 gas sensor operating at room temperature based on SnO_2/MWCNTs composite. *Sens. Actuator B-Chem.*, **2008**, *129*, 888-895.

[20] Mun, S.; Chen, Y.; Kim, J. Cellulose-titanium dioxide-multiwalled carbon nanotube hybrid nanocomposite and its ammonia gas sensing properties at room temperature. *Sens. Actuator B-Chem.*, **2012**, *171*, 1186-1191.

[21] Khorami, H.A.; Eghbali, A.; Keyanpour-Rad, M.; Vaezi, M.R.; Kazemzad, M. Ammonia sensing properties of (SnO_2-ZnO)/polypyrrole coaxial nanocables. *J. Mater. Sci.*, **2014**, *49*, 685-690.

[22] Mendoza, F.; Hernandez, D. M.; Makarov, V.; Febus, E.; Weiner, B.R.; Morell, G. Room temperature gas sensor based on tin dioxide-carbon nanotubes composite films. *Sens. Actuator B-Chem.*, **2014**, *190*, 227-233.

[23] Wang, J.; Zhou, J.G.; Fang, H.T.; Sham, T.K.; Karunakaran, C.; Lu, Y.S.; Cooper, G.; Hitchcock, A.P. Effect of humidity on individual SnO_2 coated carbon nanotubes studied by *in situ* STXM. *J. Electron. Spectrosc. Relat. Phenom.*, **2011**, *184*, 296-300.

[24] Leghrib, R.; Felten, A.; Pireaux, J.J.; Llobet, E. Gas sensors based on doped-CNT/SnO_2 composites for NO_2 detection at room temperature. *Thin Solid Films*, **2011**, *520*, 966-970.

[25] Wu, R.J.; Wu, J.G.; Yu, M.R.; Tsai, T.K.; Yeh, C.T. Use of CNT/Co_3O_4-SnO_2 in a carbon monoxide sensor operating at room temperatures. *Sens. Lett.*, **2008**, *6*, 848-851.

[26] Wisitsoraat, A.; Tuantranont, A.; Thanachayanont, C.; Patthanasettakul, V.; Singjai, P. Electron beam evaporated carbon nanotube dispersed SnO_2 thin film gas sensor. *J. Electroceram.*, **2006**, *17*, 45-49.

[27] Chen, Y.J.; Zhu, C.L.; Wang, T.H. The enhanced ethanol sensing properties of multi-walled carbon nanotubes/SnO_2 core/shell nanostructures. *Nanotechnology*, **2006**, *17*, 3012-3017.

[28] Khun, K.K.; Mahajan, A.; Bedi, R.K. SnO_2 thick films for room temperature gas sensing applications. *J. Appl. Phys.*, **2009**, *106*, 124509-1.

[29] Khun, K.K.; Mahajan, A.; Bedi, R.K. Nanostructured Sb doped SnO_2 thick films for room temperature NH_3 sensing. *Chem. Phys. Lett.*, **2010**, *492*, 119-122.

[30] Guo, X.Z.; Kang, Y.F.; Wang, L.W.; Liu, X.H.; Zhang, J.; Yang, T.L.; Wu, S.H.; Wang, S.R. Mesoporous tin dioxide nanopowders based sensors to selectively detect ethanol vapor. *Mater. Sci. Eng. C-Mater. Biol. Appl.*, **2011**, *31*, 1369-1373.

[31] Lassesson, A.; Schulze, M.; Lith, J.v.; Brown, S.A. Tin oxide nanocluster hydrogen and ammonia sensors. *Nanotechnology*, **2008**, *19*, 015502.

[32] Gyger, F.; Hübner, M.; Feldmann, C.; Barsan, N.; Weimar, U. Nanoscale SnO_2 hollow spheres and their application as a gas-sensing material. *Chem. Mater.*, **2010**, *22*, 4821-4827.

[33] Xiao Ming, Y.; Cheng Chao, L.; Ming, Z.; Quan Yi, H.; Shuang, L.; Qiu Hong, L.; Li Bao, C.; Tai Hong, W. SnO_2 monolayer porous hollow spheres as a gas sensor. *Nanotechnology*, **2009**, *20*, 455503.

[34] Chen, Z.; Pan, D.; Zhao, B.; Ding, G.; Jiao, Z.; Wu, M.; Shek, C.-H.; Wu, L.C.M.; Lai, J.K.L. Insight on fractal assessment strategies for tin dioxide thin films. *ACS Nano*, **2010**, *4*, 1202-1208.

[35] Guokang, F.; You, W.; Meng, H.; Zhiyuan, L.; Guang, L. Synthesis of flowerlike nano-SnO_2 and a study of its gas sensing response. *Measur. Sci. Technol.*, **2011**, *22*, 045203.

[36] Li, F.; Chen, L.Y.; Chen, Z.Q.; Xu, J.Q.; Zhu, J.M.; Xin, X.Q. Two-step solid-state synthesis of tin oxide and its gas-sensing property. *Mater. Chem. Phys.*, **2002**, *73*, 335-338.

[37] Srivastava, A.; Jain, K.; Rashmi; Srivastava, A.K.; Lakshmikumar, S.T. Study of structural and microstructural properties of SnO_2 powder for LPG and CNG gas sensors. *Mater. Chem. Phys*., **2006**, *97*, 85-90.

[38] Firooz, A.A.; Mahjoub, A.R.; Khodadadi, A.A. Effects of flower-like, sheet-like and granular SnO_2 nanostructures prepared by solid-state reactions on CO sensing. *Mater. Chem. Phys*., **2009**, *115*, 196-199.

[39] Liu, S.Q.; Xie, M.J.; Li, Y.X.; Guo, X.F.; Ji, W.J.; Ding, W.P. Synthesis and selective gas-sensing properties of hierarchically porous intestine-like SnO_2 hollow nanostructures. *Mater. Chem. Phys.*, **2010**, *123*, 109-113.

[40] Bamsaoud, S.F.; Rane, S.B.; Karekar, R.N.; Aiyer, R.C. SnO_2 film with bimodal distribution of nano-particles for low concentration hydrogen sensor: Effect of firing temperature on sensing properties. *Mater. Chem. Phys.*, **2012**, *133*, 681-687.

[41] Varghese, O.K.; Kichambre, P.D.; Gong, D.; Ong, K.G.; Dickey, E.C.; Grimes, C.A. Gas sensing characteristics of multi-wall carbon nanotubes. *Sens. Actuator B-Chem.*, **2001**, *81*, 32-41.

[42] Bittencourt, C.; Felten, A.; Espinosa, E.H.; Ionescu, R.; Llobet, E.; Correig, X.; Pireaux, J.J. WO_3 films modified with functionalised multi-wall carbon nanotubes: Morphological, compositional and gas response studies. *Sens. Actuator B-Chem.*, **2006**, *115*, 33-41.

[43] Carp, O.; Visinescu, D.; Patrinoiu, G.; Tirsoaga, A. Green synthetic strategies of oxide materials: Polysaccharides-assisted synthesis. PART IV. Alinate-assisted synthesis of nanosized metal oxides. *Rev. Roum. Chim.*, **2011**, *56*, 901-906.

[44] Carp, O.; Visinescu, D.; Patrinoiu, G.; Tirsoaga, A.; Paraschiv, C.; Tudose, M. Green synthetic strategies of oxide materials: Polysaccharides-assisted synthesis. I. Polysaccharides roles in metal oxides synthesis. *Rev. Roum. Chim.*, **2010**, *55*, 705-709.

[45] Visinescu, D.; Papa, F.; Ianculescu, A.C.; Balint, I.; Carp, O. Nickel-doped zinc aluminate oxides: starch-assisted synthesis,

structural, optical properties, and their catalytic activity in oxidative coupling of methane. *J. Nanoparticle Res.*, **2013**, *15*, 1456.

[46] Visinescu, D.; Tirsoaga, A.; Patrinoiu, G.; Tudose, M.; Paraschiv, C.; Ianculescu, A.; Carp, O. Green synthetic strategies of oxide materials: Polysaccharides-assisted synthesis PART II. Starch-assisted synthesis of nanosized metal-oxides. *Rev. Roum. Chim.*, **2010**, *55*, 1017.

[47] Mahadeva, S.K.; Kim, J. Conductometric glucose biosensor made with cellulose and tin oxide hybrid nanocomposite. *Sens. Actuator B-Chem.*, **2011**, *157*, 177-182.

[48] Yun, S.; Kim, J. Multi-walled carbon nanotubes-cellulose paper for a chemical vapor sensor. *Sens. Actuator B-Chem.*, **2010**, *150*, 308-313.

[49] Hong, S.J.; Jun, H.; Borse, P.H.; Lee, J.S. Size effects of WO_3 nanocrystals for photooxidation of water in particulate suspension and photoelectrochemical film systems. *Inter. J. Hydr. Energy*, **2009**, *34*, 3234-3242.

[50] Callone, E.; Carturan, G.; Ischia, M.; Sicurelli, A. Nanometric oxides from molecular precursors in the presence of starch: Coatings of glass with these oxides in silica sols. *J. Mater. Res.*, **2006**, *21*, 1726-1737.

[51] Nehru, L.; Swaminathan, V.; Sanjeeviraja, C. Photoluminescence studies on nanocrystalline tin oxide powder for optoelectronic devices. *Am. J. Mater. Sci.*, **2012**, *2*, 6-10.

[52] Mishra, D.; Srivastava, A.; Srivastava, A.; Shukla, R.K. Bead structured nanocrystalline ZnO thin films: Synthesis and LPG sensing properties. *App. Surf. Sci.*, **2008**, *255*, 2947-2950.

[53] Ghosh, A.; Sharma, R.; Ghule, A.; Taur, V.S.; Joshi, R.A.; Desale, D.J.; Gudage, Y.G.; Jadhav, K.M.; Han, S.-H. Low temperature LPG sensing properties of wet chemically grown zinc oxide nanoparticle thin film. *Sens. Actuator B-Chem.*, **2010**, *146*, 69-74.

[54] Ghule, K.; Ghule, A.V.; Liu, J.-Y.; Ling, Y.-C. Microscale size triangular gold prisms synthesized using Bengal Gram beans (*Cicer arietinum* L.) extract and $HAuCl_4 \cdot 3H_2O$: A green biogenic approach. *J. Nanosci. Nanotechnol.*, **2006**, *6*, 3746-3751.

[55] Khairou, K.S. Kinetics and mechanism of the non-isothermal decomposition: I. Some divalent cross-linked metal-alginate ionotropic gels. *J. Therm. Anal. Calor.*, **2002**, *69*, 583-588.

[56] Zohuriaan, M.J.; Shokrolahi, F. Thermal studies on natural and modified gums. *Polym. Test.*, **2004**, *23*, 575-579.

[57] Korotcenkov, G.; Tolstoy, V.; Schwank, J. Successive ionic layer deposition (SILD) as a new sensor technology: synthesis and modification of metal oxides. *Meas. Sci. Technol.*, **2006**, *17*, 1861-1869.

[58] Niesen, T.P.; De Guire, M.R. Review: Deposition of ceramic thin films at low temperatures from aqueous solutions. *J. Electroceram.*, **2001**, *6*, 169-207.

[59] Wagh, M.S.; Jain, G.H.; Patil, D.R.; Patil, S.A.; Patil, L.A. Modified zinc oxide thick film resistors as NH_3 gas sensor. *Sens. Actuator B-Chem.*, **2006**, *115*, 128-133.

[60] Betty, C.A.; Choudhury, S.; Girija, K.G. Discerning specific gas sensing at room temperature by ultrathin SnO_2 films using impedance approach. *Sens. Actuator B-Chem.*, **2012**, *173*, 781-788.

[61] Ghosh, A.; Ghule, A.; Sharma, R. In: *Effect of Cu doping on LPG sensing properties of soft chemically grown nano-structured ZnO thin film*, J. Phys.: Confer. Seri., IOP Publishing: **2012**; p. 012022.

[62] Vaezi, M.R.; Sadrnezhaad, S.K. Gas sensing behavior of nanostructured sensors based on tin oxide synthesized with different methods. *Mater. Sci. Eng. B*, **2007**, *140*, 73-80.

[63] Mishra, S.; Ghanshyam, C.; Ram, N.; Singh, S.; Bajpai, R.; Bedi, R. Alcohol sensing of tin oxide thin film prepared by sol-gel process. *Bull. Mater. Sci.*, **2002**, *25*, 231-234.

[64] Rout, C. S.; Hegde, M.; Govindaraj, A.; Rao, C. Ammonia sensors based on metal oxide nanostructures. *Nanotechnology*, **2007**, *18*, 205504.

[65] Deshmukh, R.G.; Badadhe, S.S.; Vaishampayan, M.V.; Mulla, I. Facile synthesis and gas sensing properties of nanotriangular tin oxide. *Mater. Lett.*, **2008**, *62*, 4328-4331.

[66] Duc Hoa, N.; Van Quy, N.; Suk Cho, Y.; Kim, D. Nanocomposite of SWNTs and SnO_2 fabricated by soldering process for ammonia gas sensor application. *Phys. Status Solidi A*, **2007**, *204*, 1820-1824.

Received: June 17, 2014 **Revised: October 15, 2014** **Accepted: October 31, 2014**